

THE EFFECTS OF SUPPORTS ON THE FLOW BEHIND A BODY

P. Rebuffet

Translation of "Effets de supports sur l'écoulement à l'arrière d'un corps, AGARD, Paris, France, Report 302 (Presented at La Réunion sur les Effets des Interactions en Soufflerie du Groupe de Trail, AGARD, Rhode St. Genese, Belgium 2-5 Mar 1959), March 1959, pp 1-31



(NASA-TM-77073) THE EFFECTS OF SUPPORTS ON
THE FLOW BEHIND A BODY (National Aeronautics
and Space Administration) 47 p
HC A03/MF A01

N83-33909

CSCL 14B

Unclass
36097

G3/09

STANDARD TITLE PAGE

1. Report No. NASA TM-77073	2. Government Accession No.	3. Recipient's Catalog No.	
4. Title and Subtitle THE EFFECTS OF SUPPORTS ON THE FLOW BEHIND A BODY		5. Report Date MAY 1983	
		6. Performing Organization Code	
7. Author(s) P. Rebuffet		8. Performing Organization Report No.	
		10. Work Unit No.	
9. Performing Organization Name and Address Leo Kanner Associates Redwood City, CA 94063		11. Contract or Grant No. NAS-3541	
		13. Type of Report and Period Covered Translation	
12. Sponsoring Agency Name and Address National Aeronautics and Space Administration, Washington, D.C. 20546		14. Sponsoring Agency Code	
15. Supplementary Note. Translation of "Effets de supports sur l'écoulement à l'arrière d'un corps, AGARD, Paris, France, Report 302 (Presented at La Réunion sur les Effets des Interactions en Soufflerie du Groupe de Trail, AGARD, Rhode St. Genese, Belgium 2-5 Mar 1959), March 1959, pp 1-31 (N80- 71569)			
16. Abstract This report studies two cases in a supersonic flow with a turbulent boundary layer in order to determine the effects of supports on models with a flat base. The first concerns the effect of various obstacles situated upstream of the two-dimensional base, at Mach 2. The second relates to a body of revolution passing through the throat of the jet from upstream to downstream. The interference of obstacles simulating supporting masts is examined for the base, both bare and with a sting, at Mach 1.94. Without any support, the drag of a conical-cylindrical body of revolution was measured by means of the ONERA magnetic suspension. The interference of various stings was studied at Mach 2.4 with a laminary boundary layer and with a separated turbulent boundary layer. The mechanism of the interference of a sting, progressively approached axially to the base, was determined.			
17. Key Words (Selected by Author(s)) BASE FLOW/SUPRSONIC WIND TUNNELS/ SUPPORTS/SUSPENDING (HANGING)/ FLAT SURFACES/LAMINAR BOUNDARY LAYER/MAGNETIC SUSPENSION/SUPERSONIC FLOW/TURBULENT BOUNDARY LAYER/		18. Distribution Statement Unclassified-Unlimited	
19. Security Classif. (of this report) Unclassified	20. Security Classif. (of this page) Unclassified	21. No. of Pages	22.

SUMMARY

With a view to determining the effects of supports on models with a flat base, two cases are examined, in a supersonic flow with a turbulent boundary layer. The first concerns the effect of various obstacles situated upstream of the two-dimensional base, at Mach 2. The second relates to a body of revolution passing through the throat of the jet from upstream to downstream. The interference of obstacles simulating supporting masts is examined for the base, both bare and with a sting, at Mach 1.94. Without any support, the drag of a conical-cylindrical body of revolution was measured by means of the ONERA magnetic suspension. The interference of various stings was studied at Mach 2.4 with a laminar boundary layer and with a separated turbulent boundary layer. The mechanism of the interference of a sting, progressively approached axially to the base, was determined.

/ii*

*Numbers in the margin indicate pagination in the original text.

ANNOTATIONS

M_o	Mach number
q_o	Kinetic pressure ($= \frac{1}{2} \rho_o v_o^2$)
R	Reynolds number
h	Height of the parallel plane ressaut (step)
l	Distance from the tip of an obstacle to the step
D	Diameter of the cylindrical body ($= 2R$)
d	Sting diameter
δ	Conventional thickness of the boundary layer
p_o	Pressure of a nondisturbed flow (at infinity)
p_c	Base pressure
p_d	Pressure measured on the upstream face of the sting
K_{pc}	Base pressure coefficient ($= (p_c - p_o)/q_o$)
K'_{pc}	Ratio of base pressure coefficient to local conditions
X	Axial force measured with the magnetic suspension
C_x	Resistance coefficient ($= X/(a_o S)$)
C_{xc}	Base resistance coefficient ($= -K_{pc}$)
S	Straight section region of the conical-cylindrical mock-up (reference surface)

TABLE OF CONTENTS

	PAGE
SUMMARY	i
LIST OF FIGURES	iii
ANNOTATIONS	iv
1. INTRODUCTION	1
2. INTERFERENCE OF OBSTACLES ON A BASE IN A SUPERSONIC PARALLEL PLANE FLOW	3
2.1 Experimental Mounting	3
2.2 Results	4
3. INTERFERENCES OF OBSTACLES ON THE BASE OF A BODY OF REVOLUTION	6
3.1 Experimental Mounting	7
3.2 Characteristics of the Flow With An 'Upstream Sting'	8
3.3 Interference of A Downstream Sting	9
3.4 Fin Interferences	11
3.5 Observations	12
4. MEASUREMENT OF THE RESISTANCE OF A BODY OF REVOLUTION WITHOUT ANY EQUIPMENT SUPPORT	13
4.1 Reminder of the Magnetic Suspension Principle	13
4.2 Magnetic Suspension Used	15
4.3 Supersonic Test Section	15
4.4 Experimental Process	16
4.5 Results Pertaining To A Conical-Cylindrical Mock-Up	17
5. CONCLUSIONS	24
REFERENCES	25
FIGURES	
DISTRIBUTION	

LIST OF FIGURES

PAGE

- Figure 1 Interactions on a base in a parallel plane flow ($M_0 = 2$)
- Figure 2 Interactions of obstacles on the base of a body of revolution
- Figure 3 Local Mach numbers on the generatrices of bodies of revolution
- Figure 4 Interference of a sting on the base of a body of revolution with a turbulent boundary layer (equivalent $R_x = 3.5 \times 10^6$)
- Figure 5 Interference of a finned support on the base of a body of revolution
- Figure 6 Strioscopies of the flow for different fin positions
- Figure 7 Diagram of the ONERA magnetic suspension
- Figure 8 Supersonic test section with magnetic suspension
- Figure 9 Experimental mock-up and sting
- Figure 10 Interference of a sting
- Figure 11 Variation of the pressure measured at the tip of a sting
- Figure 12 Interference of a sting on the coefficient of resistance C_x
- Figure 13 Interference of a sting on the base pressure
- Figure 14 Results obtained on the conical-cylindrical mock-up
- Figure 15 Pressure coefficient of the base as a function of the relative sting diameter
- Figure 16 Effect of the Reynolds number

EFFECTS OF SUPPORTS ON THE FLOW BEHIND A BODY

/1

P. Rebuffet
Assistant Scientific Director of Aerodynamics
Onera, France

1. INTRODUCTION

The method of linking the test equipment and the model to be studied in a wind tunnel should be selected by paying special attention to the interferences generated by the presence of the supports.

This problem which has cropped up constantly since the beginning of aerodynamic experimentation has been the subject matter of numerous critical studies.

It is needless to say that simple conclusions cannot be given when so many parameters are to be taken into consideration: Mach and Reynolds range, mock-up geometry, magnitudes to be measured, etc.

Moreover, the arrangements generally adopted most often result in a compromise.

Overall measurements are taken to demonstrate the interference of supports in a specific case; they are relative to the coefficients of forces and moments.

To define the interference process, experiments of an analytical nature are required. The recording of local pressures gives interesting elements, but is often a difficult operation, if it involves small-scale testing on a full-scale mock-up. For the same purpose, visualization methods contribute greatly to the understanding of the phenomena.

The visualization of fluid filaments, either within the flow, or on the wall of the mock-up is commonly practiced in the wind tunnel. Many methods adapted to the objective being investigated (investigation of separations, vortices, visualization of the transition) have been developed for many years and adapted to ever increasing ranges.

This report is offering a few comments on the results pertaining to the interference of supports on the flow of at the base of a body in a supersonic flow. These results were obtained on the occasion of fundamental investigations carried out in small wind tunnels of the Fluid Mechanics Laboratory at ONERA.

The first test was performed on a flat base in a parallel plane flow. The second test was performed on a body of revolution using a mounting called "upstream sting", used for jet studies. The sting passes through the throat of the jet nozzle from upstream to downstream and has no support in the supersonic region of the flow.

In both cases, the studies were conducted with a turbulent boundary layer. Obstacles simulating supports were arranged upstream of the base. An axial sting was also placed downstream of the body of revolution. /2

In the third study, we present the results obtained using the ONERA magnetic suspension.

The drag of a body of revolution was measured with excellent precision in a supersonic flow, without any equipment support.

This suspension made it possible to study the mechanism of the interference caused by a sting progressively approaching the base and to define, within the test

conditions ($M = 2.4$, $R = 1.4 \times 10^6$), the "minimum interference distance" for different sting diameters with a laminar and turbulent boundary layer.

2. INTERFERENCE OF OBSTACLES ON A BASE IN A SUPERSONIC PARALLEL PLANE FLOW

When the experimental study was performed on the phenomena governing the base pressure in a two-dimensional flow, it seemed interesting to demonstrate the influence of an obstacle located upstream from the base.

The study was carried out by Mr. Sirieix, in the case of a turbulent boundary layer approaching an abrupt separation provided at the wall of parallel plane jet nozzle, at Mach number $M = 2$ (Reference 1).

2.1 Experimental Mounting

The mounting was set up in a small basic research wind tunnel, using a half-nozzle $M = 3$, test section 80 mm x 80 mm, pressure generation 1 atmosphere. Figure 1 shows the general arrangements adopted: upper fixed nozzle, lower platform (indistinguishable from the plane of symmetry of the full nozzle) which can slide along its plane and provided with a separation shaped like the step of a stair, of height $h = 20$ mm.

The platform was equipped with pressure pickups upstream from the separation, on the base of the latter and downstream. These pickups were arranged along the plane of symmetry of the platform and also laterally, upstream from the step in order to determine the uniformity of the flow approaching the step.

Three types of obstacles (figure 1) were studied. Their distance l from the step varies with the platform displacement. These obstacles generate fields of disturbances which vary with their nature and intensity.

Obstacle 1 is a flat plate 3 mm thick, parallel to the side walls of the test section and passing through the throat of the jet nozzle from upstream to downstream. It has a base with a sharp edge and generates a relatively thick slip stream.

Obstacle 2 is made of the same plate and its trailing edge is rendered sharp (total dihedral of 10°). The disturbances are essentially characterized by the*

Obstacle 3 is a 3 mm cylinder whose diameter generates a more complex and intense field of disturbances, with a thin slip stream. /3

2.2 Results

2.2.1 The boundary layer approaching the step, without any obstacle upstream, is turbulent. Its conventional thickness is $\delta = 3.1$ mm. This thickness should be obtained on a flat plate at $M = 2$, uniform pressure p_o , turbulent boundary layer, for Reynolds number $R_x = 1.8 \times 10^6$ where x is the length of the equivalent flat plate (equivalent Reynolds number).

2.2.2 The following results concern the base pressure occurring in stagnant water, upstream from the step.

The pressure measured on the base using different pickups in the vicinity of the plane of symmetry is virtually uniform. We will represent this pressure by p_c , with p_o being the pressure of the nondisturbed flow.

Without any obstacle, $p_c/p_o = 0.33$ (figure 1). This value coincides satisfactorily with the experimental results.

When the tip of an obstacle is situated at a distance l upstream from the base, the base pressure changes appreciably. Its value depends on the obstacle's distance. For all values tested with parameter l/h , an interference occurs.

This interference is due to the disturbances generated by the obstacle. This field locally modifies the circumstances for the reattachment of the step downstream. Consequently, the base pressure which reaches a mean value, obviously depends on the transversal dimension of the flow.

The interference caused by the obstacle changes sign, depending on whether the field of disturbances is essentially characterized by compressions or expansions relative to the pressure level p_0 which is initially uniform upstream from the step.

Accordingly, in the case of the cylindrical obstacle (figure 1), the measured base pressure exceeds the reference pressure occurring without an obstacle by 30%: in the range of variation considered for parameter l/h , the shock wave of the cylinder is reflected by the side walls. It concerns the flow approaching the step and also the stagnant water region downstream from the step.

When the cylinder gets close to the step, the difference on p_c/p_0 decreases, the disturbance field affects a smaller area of the flow and part of the reflected disturbances move downstream from the interference domain.

The results obtained with flat obstacles, with or without sharp edges, are very similar: the base pressure p_c is 15% lower than the reference pressure. It varies little as a function of the distance of the plate's tip to the step. It is essentially the field of overspeeds caused by the expansions which condition the interference. The effect of a larger slip stream in the case of a sharp-edged plate is not clearly distinguishable.

2.2.3 In conclusion, the presence of different obstacles arranged upstream from a step in a two-dimensional flow, with turbulent boundary layer, produces an interference which noticeably affects the pressure at the base. The sign of the interference depends essentially on the nature of the obstacle.

/4

Although the numerical values obtained with the different obstacles depend essentially on the transversal dimension of the parallel plane flow, this experiment shows the importance of the effect of a side support located upstream from a base.

3. INTERFERENCES OF OBSTACLES ON THE BASE OF A BODY OF REVOLUTION

The study in a supersonic wind tunnel of a flow behind an aircraft or spacecraft faces numerous obstacles if we want to represent the jet effects.

Among these difficulties, two of them are especially important: the supply to the ejection nozzle must be provided in such a manner that the flow in the vicinity of the base is not disturbed. The waves issuing in front of the mock-up must not interact with the base after reflecting on the walls of the test section.

One solution offered, especially with for fundamental studies in wind tunnels with small dimensions, consists of supporting the rear body of the aircraft or spacecraft by a sting passing through the throat of the jet nozzle from upstream to downstream. This arrangement may be retained only to study the base phenomena in the presence of a turbulent boundary layer created.

The mounting can be made correctly and easily in the

in the case of a cylindrical body placed inside a specially designed revolving nozzle.

In the case of a two-dimensional nozzle, the running tube which is contoured to the bulkhead of the body under consideration can be 'fixed' to give the 'upstream sting' the shape of this running tube.

Such an arrangement, recently created and now being studied, should make large dimensions permissible, but the boundary layer formed in the real fluid could be affected by the nonuniform pressure at the periphery of a straight section of the body and therefore cause disturbances within the nozzle.

An approximated solution, acceptable for small Mach numbers, may be retained: it consists of using a cylindrical 'upstream sting' by limiting the sting's diameter so that the relative dimensions or clearance of the nozzle remain small.

3.1 Experimental Mounting

The mounting with cylindrical upstream sting was used by Mr. Sierieix in a small test wind tunnel at ONERA's Fluid Mechanics Laboratory; it is now being perfected.

The nozzle used has a square section of 120 mm per side, the theoretical Mach number is 1.95 (generating pressure 1 at, generating temperature 20°C).

/5

The upstream sting has a diameter of 28 mm, or a relative clearance of 4.3%. It can receive different tips.

One of them, which extends the sting, has a straight base equipped with pressure intakes on one of its generatrices and on the base in an angular sector of 60° (figure 2). The upstream sting's rotation about its axis makes it possible to explore the pressure distribution along the circumference of the cylinder and over the entire surface of the base.

A second tip, also equipped with pressure intakes, bears two fins (figure 2) simulating a lateral support. Sliding elements make it possible to vary the distance l from the leading edge of these fins to the base, l/D remaining between 0 and 1.5. These fins may be placed in the plane of symmetry of the nozzle or perpendicular to this plane.

A sting (figure 2) may be fastened to the tip of the upstream sting in order to simulate a mounting with axial sting, with and without fin.

3.2 Characteristics of the Flow With An 'Upstream Sting'

In the rhombus of measurements, with the upstream sting in position, and without any support, the static pressures were measured on the side walls of the nozzle and on the generatrices of the cylindrical body.

The strioscopies of the flow do not indicate any large disturbances. On the cylindrical body, in the vicinity of the base, the differences on M reach ± 0.015 , the mean Mach number being 1.94 (figure 3).

In the plane of the base, within the free flow, these differences are generally between ± 0.01 and 0.02.

The measurement of the pressure on numerous points of the base, performed by rotating the sting about its axis, brings to light that the base pressure is nonuniform, and that the relative pressure differences may be as great as ± 0.06 , which is greater than those appearing on the generatrices of the cylinder upstream from the base.

These differences are much smaller ($\leq \pm 0.02$) when a downstream sting is mounted on the base (provided that the ratio d/D is greater than 0.5) or when the fins are located upstream from the base.

On a generatrix of the cylindrical body situated in a horizontal plane, upstream from the bare base, the turbulent boundary layer has a conventional thickness $\delta = 4$ mm; the equivalent Reynolds number, calculated with a completely turbulent boundary layer in a flow at $M_0 = 1.94$, uniform pressure p_0 , is $R_x = 3.5 \times 10^6$.

3.3 Interference of a Downstream Sting

The facilities offered by the mounting made it possible to test a fairly large number of stings, with the diameter d/D varying from 0.05 to 0.95.

Accounting for the uniformity of the base pressure mentioned above, the base pressure was measured in an angular sector where there is little pressure variation. This sector was retained in the rest of the tests, with bare base or with supports.

/6

The results obtained are shown in figure 4. We have shown the ratio p_c/p_0 as a function of the relative diameter d/D of the sting, where p_c is the mean base pressure. A second curve expresses the same results in the form of the base pressure coefficient $K'_{pc} = (p_c - p_0) / (\frac{1}{2} \gamma p_0 M_0^2)$.

For comparison, we matched this curve with that deduced from reference 3, by correlating the base pressure coefficient with the local conditions of the flow immediately upstream from the base.

The curve obtained, at Mach number $M = 1.94$, equivalent $R_x = 3.5 \times 10^6$, shows that the base pressure is not greatly affected as long as the sting diameter does not exceed 0.3.

When the relative sting diameter exceeds this value, the base pressure decreases slowly, then quickly, and reaches a minimum d/D between 0.8 and 0.9. The base pressure is therefore reduced by 18% by the interference.

The base pressure then increases very quickly and reaches p_0 when d/D is in the vicinity of 1.

The strioscopic visualization of the flow shows the following points:

Without a sting, the very progressive and extensive recompression of the flow occurs through the waves which focalize at an appreciable distance from the slip stream. The slip stream diameter is about 0.7 D , including the boundary layer.

A sting having a relative diameter of less than or equal to 0.3, in the presence of a base, does not greatly affect the wave system as the waves focalize much closer to the edges of the slip stream.

When the diameter increases even more, a recompression wave appears and its intensity increases with d/D , the distance of the reattachment point decreases very rapidly and the boundary layer on the sting becomes much thinner. The most favorable reattachment conditions lead to lower base pressure values, owing to a pressure jump at the highest reattachment point.

When the sting diameter approaches that of the base, the value of the distance from the reattachment point at the base becomes low with respect to the value of the boundary layer thickness.

3.4 Fin Interference

The results shown in figure 5 demonstrate the interference of the fins defined above and which are located at various distances l/D from the base.

The essential remark lies in the fact that these interferences are numerically very different when the base is bare or when the downstream sting is attached to it. They are small in this latter configuration.

The interference is moreover quite different in the case where the fins are in a horizontal or vertical plane. The reflections of the leading edge and trailing edge fin shocks which are generated on the nozzle walls or side walls respectively do not seem to justify this difference which can be partially due to the dissymetries of the flow.

The strioscopies in figure 6 make it possible to determine the mode of interference of the fins with and without a sting.

Without a sting and for the farthest position from the fins, $l/D = 1.5$, the shock wave issuing from the leading edge and reflected by the walls reaches the boundary of the slip stream of the base at a distance from the base equal to about $1.5 D$ and provokes a large interference on the base pressure.

With a downstream sting at the base ($d/D = 0.5$), the

/7

The reattachment on the sting occurs at a short enough distance from the base so that the reflected shock wave does not interfere appreciably with the base pressure.

This comparison thus gives a good idea, to a certain extent, of the interference caused by the specific field of the fins and by their slip stream, excluding the effect of the reflections.

With a sting, the p_c varies little and varies slowly with l/D which shows that the interference caused by the fin field and its slip stream is moderate.

Conversely, the interference caused by the reflected leading edge and trailing edge shock waves is large and varies with l/D : it modifies the conditions for the reattachment of the jet. This is another aspect of the interference of a finned support in a wind tunnel with small dimensions.

3.5 Observations

The experiments which we have just described, pertaining to the interference effects of supports on the base pressure, have no other purpose than to draw one's attention to a few points:

1 upstream sting type mounting is convenient for the study of base problems in the absence of any support. It seems particularly suitable for basic investigations in small wind tunnels.

The quality of the flow must be excellent in order to obtain a uniform pressure at the base. If this pressure

is measured on a single point, then irregularities can be concealed.

The disturbances affecting the domain upstream from the jet's reattachment disturbs the base pressure, which confirms the usual rule of preventing any disturbance from affecting a bare base over a length of several diameters downstream from the base.

The effect of a support is not only a function of its position, but also of the dimensions of the test section and of the Mach number, owing to the reflections on the walls.

4. MEASUREMENT OF THE RESISTANCE OF A BODY OF REVOLUTION WITHOUT ANY EQUIPMENT SUPPORT

/8

For several years, ONERA has been developing a magnetic suspension device of a wind tunnel mock-up for the purpose of testing a body without any equipment support.

This suspension thus enables the resistance of a mock-up to be obtained without any interference and makes it possible to study the variation of the mock-up when a support such as an axial type, for example, progressively approaches the base.

4.1 Reminder of the Magnetic Suspension Principle

The magnetic suspension principle studied by Mr. Tournier and P. Laurenceau is given in Reference 4.

Let us simply recall that the mock-up, made of soft steel, is set up parallel to the speed and its position is stabilized by the electromagnetic actions. The arrangements adopted are described below (figure 7):

A horse-shoe electromagnet has 2 coils E_1 and E_2 , supplied separately and designed to support the mock-up. The lines of forces of the magnetic field created by the electromagnet close up inside the mock-up which becomes magnetized by induction.

Below the coils E_1 and E_2 , two horizontal light beams emitted by projectors p_1 and p_2 are perpendicular to the axis of the mock-up and are partially hidden by it. These beams are reflected into photo-electric cells C_1 and C_2 by mirrors M_1 and M_2 .

This device sets the height position of the mock-up and introduces the required damping time using the electric circuit described in Reference 4: any change in the position of the mock-up modifies the luminous flux received by the cells C_1 and C_2 whose currents control the currents passing through coils E_1 and E_2 respectively.

A winding E_3 around the test section and upstream from the mock-up makes it possible to balance the resistance of the air. The current in this coil is controlled by the device P_3 , M_3 , C_3 which sets the axial position of the mock-up, the backward motion of which hides the corresponding light beam.

In similar conditions, a horizontal electromagnet has 2 coils E_4 and E_5 which position the mock-up along the horizontal plane using the sets P_4 , M_4 and P_5 , M_5 , C_5 and dampens its transversal oscillations (lateral stabilization).

Finally, if a mock-up having no axis of symmetry is used, the rolling angle may be cancelled using an appropriate device.

In summary, the magnetic suspension serves to stabilize the position of a mock-up without any equipment support and to measure the stresses applied to the mock-up.

The application of this method to experiments in a supersonic flow, which is the subject matter of the text below, was limited to a mock-up revolving at zero incidence, without being confronted with the problem of eliminating the mechanical interferences between the different components of the aerodynamic torque, or to account for it via the appropriate settings.

/9

4.2 Magnetic Suspension Used

The general arrangements of the suspension used are given in Reference 4.

This suspension is adapted to mock-ups of a certain size, the length and diameter cannot be less than about 120 and 11 mm respectively, unless certain elements are modified and new settings are made*.

4.3 Supersonic Test Section

An application of the magnetic suspension in a supersonic flow and the corresponding aerodynamic studies were performed by J. Mirande [5] at the ONERA Fluid Mechanics Laboratory.

A test section $M = 2.4$ was specially built (figure 8). It is not necessarily made with any steel element and the use of metallic parts is limited as far as possible.

*The transonic test section in which the tests described in Reference 4 were conducted was slightly too small for the body tested.

The nozzle was made in plexiglass to enable the light beams to pass through and the mock-up to be observed. The convergent and divergent are built in a wood coated with bakelite. The sting supports are in brass.

The nozzle has a section 85 mm by 85 mm. The Mach number is equal to 2.42 ± 0.02 in the measuring rhombus.

4.4 Experimental Process

4.4.1 Setting of the Magnetic Suspension

The magnetic suspension being in operation, while the wind tunnel is not operating, the device used for measuring the resistance is set as follows:

The mock-up is 'set' on the optical lift beams which hold it in place.

The known stresses are applied to the mock-up via a horizontal wire attached to its base, the current running through the resistance coil E_3 is recorded (or more precisely a current which is proportional to it, using a sensitive galvanometer).

The resistance to be measured during the course of the experiments undertaken did not exceed about 100 grams. The settings were adjusted by increasing and decreasing values and were repeated several times, showing an accuracy of $\pm 0.5g$.

4.4.2 Energizing the Wind Tunnel

The mock-up must be held in place with an auxiliary support throughout this operation*, otherwise it would

*In a small blast wind tunnel, $M = 7$, with an empty tank downstream from the nozzle, the energizing operation can be performed with the mock-up held by electromagnetic actions alone.

escape the action of the magnetic suspension under the effect of the vibrations it is subjected to.

To prevent any flow instability during the nozzle energizing phase, the mock-up base is capped by a sting-shaped hollow support. A tube sliding in the support pushes down on the base to hold the mock-up in position.

Once the energization is achieved, a current is applied to the lift and lateral stabilization electromagnets. The sliding tube is moved back downstream, the depression on the base is removed and the resistance electromagnet is initiated.

The auxiliary support is retractable and can therefore be moved backward: the mock-up becomes charged by the magnetic suspension.

Virtually similar operations are performed in reverse order before uncharging the system. The auxiliary support again holds the mock-up in position to avoid any drop in the nozzle.

4.4.3 Adjusting the Angle of Attack During Operation

The mock-up is adjusted using an optical sight at zero angle of attack (mock-up body parallel to the axis of the nozzle) with projectors P_1 and P_2 which can be placed parallel to each other.

4.5 Results Pertaining To A Conical-Cylindrical Mock-Up

4.5.1 Mock-Up

The mock-up studied, with a diameter of $D = 12$ mm, is defined in figure 9. It was tested as such, the surface

being carefully polished, and also with a transition triggering device: pitch area 0.3 mm, depth 0.2 mm.

Several copies of these mock-ups, identical to the factory specifications, were made and tested.

A sliding sting that can move up to the base of the mock-up is defined in figure 9. Its front section, of diameter d , is detachable.

The distance between the tip of this interacting sting and the base (measured accurately using a telescope) could not be reduced more than 1 mm so as to not cut off the light beam which controls the current in the resistance coil.

Each of the stings offers an axial line which transmits a pressure p_d measured against a reference pressure in the vicinity of the flow pressure at infinity (ethyl-glycol manometer). The sting with the smallest diameter $d = 1$ mm offers a stop-pressure probe.

/11

When $x = 1$ mm, the pressure p_d measured by the sting can be identified with the base pressure.

4.5.2 Nature Of The Boundary Layer During The Course Of The Tests

The REynolds number R_L calculated with the length $L = 130$ mm of the mock-up is 1.4×10^6 .

Visualizations using acenaphtene sublimation showed that the boundary layer at the base of the mock-up was laminar and that it actually becomes turbulent when the transition device was used.

The same conical-cylindrical mock-up being held by an axial sting ($d/D = 0.5$), a boundary layer sounding was performed in both cases and this confirmed the nature of the boundary layer: laminar boundary layer with a thickness of 0.6 mm; separated turbulent boundary layer about 2 mm thick.

4.5.3 Interference of A Progressively Approaching Sting

Figure 10 shows the results obtained when a sting $d/D = 0.5$ progressively approaches the base of the mock-up (transition onset) and then moves backward.

The coefficient C_x of the resistance, obtained by measuring the axial force by the magnetic suspension, is shown as a function of the distance x from the sting to the base.

We see that C_x is constant for x/D is greater than or equal to 3, then experiences a negative variation when x decreases, which results in a large interference of the sting. For $x/D < 2$, C_x increases and stabilizes when x/D is less than 0.5. In this case, the sting interference: the difference between the value measured with the sting being very far away and with a sting 1 mm from the base, is positive and equal to 0.02, or about 6.3% of the resistance without interference. This interference is insignificant compared to that produced by the sting when it progressively moves away from the base*.

The pressure variation p_d transmitted by the internal canalization of the sting, measured simultaneously with the resistance, is shown in figure 10. The ratio p_d/p_o decreases rapidly, then stabilizes like C_x when x/D is greater than 0.5. The value of p_d measured 1 mm from the base

/12

*See footnote on page 20.

can be reasonably considered identical to the pressure p_c predominating in the interfered base. This gives the pressure coefficient of the base $K_{pc} = -0.124$ and the base resistance $C_{xc} = 0.124$.

Since the test mock-up has no restriction, we may ascribe the variations of C_x to that of C_{xc} and deduce from it the variation of the base pressure p_c when the sting gradually moves backward. The curve p_c/p_0 plotted in figure 10 was thus obtained. It shows that the static pressure p_d is indistinguishable from p_c when the sting moves backward up to about $x/D = 0.5$.

The difference between p_d and p_c essentially denotes the progressive downstream recompression of the base and, secondarily, the kinetic pressure effect when the sting moves out of the stagnant water.

Figure 11 shows the variation of the curves p_d/p_0 in the vicinity of the base, obtained with stings of different diameters, with laminar boundary layer and turbulent boundary layer. We may note the variations of p_d in both cases and a notable difference with the laminar boundary layer, when the test is performed again several

*The test section used with plexiglass side walls did not allow for striaoscopic visualizations of the flow. An exploration of static and dynamic pressures in the slip stream axis, with a bare base, has nevertheless shown that the slip stream was sonic on the axis at a distance x/D is congruent with 2.8 (appreciably the same distance in the laminar and turbulent boundary layers). Note simply that a sting extended in a supersonic slip stream should not cause an interference, but when the sting reaches the subsonic domain of the slip stream, it produces a recompression which propagates to the stagnant water region and tends to increase the base pressure. A negative drag variation results. The sting approaching the base creates more complex phenomena which would be interesting to define using striaoscopies.

times. This difference also detected on the overall C_x obtained with the magnetic suspension still does not exceed $\Delta C_x = \pm 0.0035$, or $\pm 1.5\%$ (laminar boundary layer, $d/D = 0.33$), a value much higher than that obtained with the magnetic suspension measurement. It therefore seems that the flow at the base is not stable when the boundary layer is laminar.

It should be noted that the length x for which p_{01} varies little correlates with the position of the point of the boundary layer reattachment on the sting (length of the stagnant water).

4.5.4 Interference Produced Using Different Stings

Several mock-ups, although built as similar as possible and used successively, the interference effects of the different stings was demonstrated not by comparing the curves C_x , but by the difference ΔC_x between C_x obtained when the sting moves backward out of the interference domain and the C_x is measured with a sting at distance x .

The curves in figure 12 show the results obtained in a laminar and in a turbulent flow. The main observations are:

The interference distance decreases when the ratio d/D decreases, but remains of the same order of magnitude in a laminar and in a turbulent flow.

The maximum ΔC_x (absolute value) remains similar in the two cases.

However, the interference with the sting moving right next to the base ($x = 1 \text{ mm}$) is much smaller with

a laminary boundary than with a turbulent boundary. In a turbulent regime, this interference is always positive when d/D is greater than or equal to 0.33. In all cases, the presence of a sting increases the resistance of the mock-up.

Figure 13 shows the same interference effects detected by the variation of the ratio p_c/p_o . The pressures p_c were obtained either by direct manometric measurement, or from the resistance measured using the magnetic suspension, where ΔC_x results from the pressure difference at the base. This description brings to light a much greater difference in a laminar than in a turbulent flow.

/13

Figure 14 gives the resistance coefficient C_x of the conical-cylindrical mock-up from overall measurements and the base resistance coefficient C_{xc} deduced by measuring the base pressures.

The resistance values obtained for $d/D = 0$ (without a sting), are $C_x = 0.237$ (laminar boundary layer) and $C_x = 0.335$ (turbulent boundary layer) respectively, each at about ± 0.002 .

It is interesting to show an approximated summary of the different terms involved in the resistance determination:

	----- Laminar Boundary Layer -----	----- Turbulent Boundary Layer -----
Pressure resistance (according to the Kopal tables)	0.096	0.096
Calculated friction resistance	0.041	0.121
Measured base resistance	<u>0.100</u>	<u>0.110</u>
Overall resistance	0.237	0.327

These values are in excellent agreement with the overall measurement performed using the magnetic suspension. Note that the friction resistance was calculated using approximated formulas (NACA REM E 5 1 H 17 and van Driest relations) by assuming in the turbulent case that a boundary layer was established as of the tip of the cone.

4.5.5 Comparison with Previous Results

Figure 15 compares the results obtained with those of Reference 3. The base pressure coefficient is correlated with local conditions.

Note that at $M = 2$, the effect of the Reynolds number is important in the case of a laminar boundary layer, as shown in figure 16 deduced from the D.A. Chapman tests, while it is virtually zero when the boundary layer is turbulent. This Reynolds effect explains the position of the ONERA curve $M = 2.4$ with respect to the curves $M = 2.9$ of NACA.

In regard to the variation of the base pressure coefficient (turbulent boundary layer) as a function of d/D (figure 15), a difference appears at high d/D values and no explanation for this can be found.

4.5.6 The results presented above show that it was possible to perform measurements in a supersonic flow at $M = 2.4$ on a body of revolution with any equipment support, using a magnetic suspension, in a laminar boundary layer and turbulent boundary layer. /14

Furthermore, this suspension made it possible to offer contributions to the study of the problem of the

interference of a sting progressively approaching a base without any auxiliary support disturbances, particularly in a laminar boundary layer.

5. CONCLUSIONS

Different obstacles located upstream from a two-dimensional base producing an interference on a base pressure whose sign depends on the nature and intensity of the disturbance field.

On a body of revolution passing through a jet nozzle from upstream to downstream without any support in the supersonic flow, relatively small disturbances may notably affect the uniformity of the pressure at the base.

In both cases, with the turbulent boundary layer at a right angle with the base, the effect of an upstream support is not only a function of its position, but also of the dimensions of the test section and of the Mach number, as a result of the reflections on the walls of the test section.

The experiment performed using the ONERA magnetic suspension made it possible to measure, without any support interferences, the resistance of a conical-cylindrical body of revolution, with excellent precision, for a laminar or turbulent boundary layer.

The interference of the different stings in the immediate vicinity of the base was studied, as well as the mode of interference of these stings, progressively approaching the base.

The minimum interference distance and the variation of this interference in magnitude and in sign were determined.

REFERENCES

1. Sireix, M., "Interferences of an obstacle on the Base pressure in a plane parallel supersonic flow ($M = 2$). Brief information, La Recherche Aeronautique, 69 (1959).
2. Love, E.S., "Base pressure at supersonic speeds on two-dimensional airfoils and on boides of revolution with and without fins having turbulent boundary layer," NACA Tehnical Note 3819, 1957.
3. Chapman, D.A., "An analysis of base pressure at supersonic velocites and comparison with experiment," NACA Report 1051, 1951.
4. Tournier, M., Laurenceau P., "Magnetic suspension of a mock-up in a wind tunnel," La Recherche Aeronautique No. 59, 1957.
5. Mirande, J., "Measurement of the resistance of a body of revolution at $M = 2.4$ using the ONERA magnetic suspension," Brief Information, La Recherche Aeronautique No. 69, 1959.

ORIGINAL PAGE IS
OF POOR QUALITY

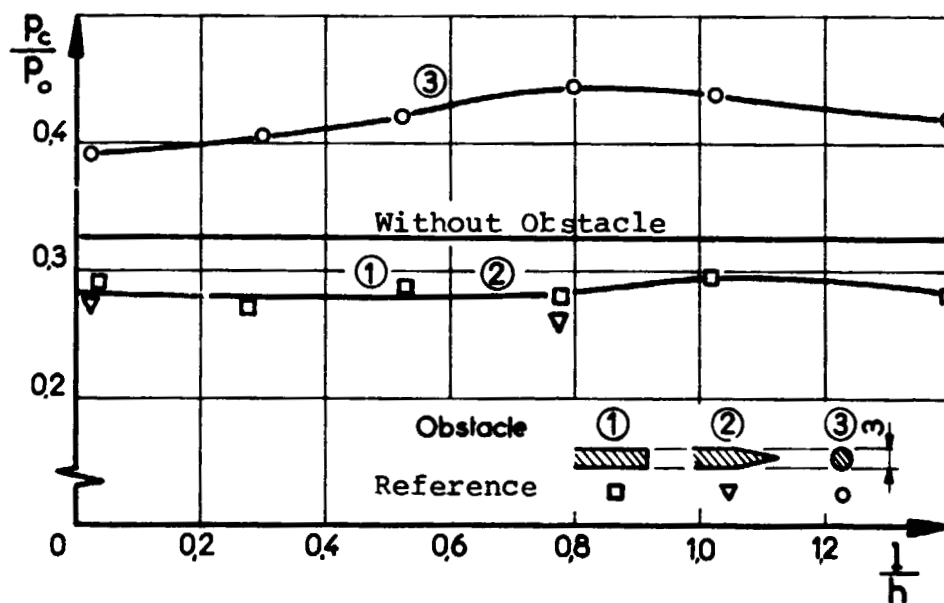
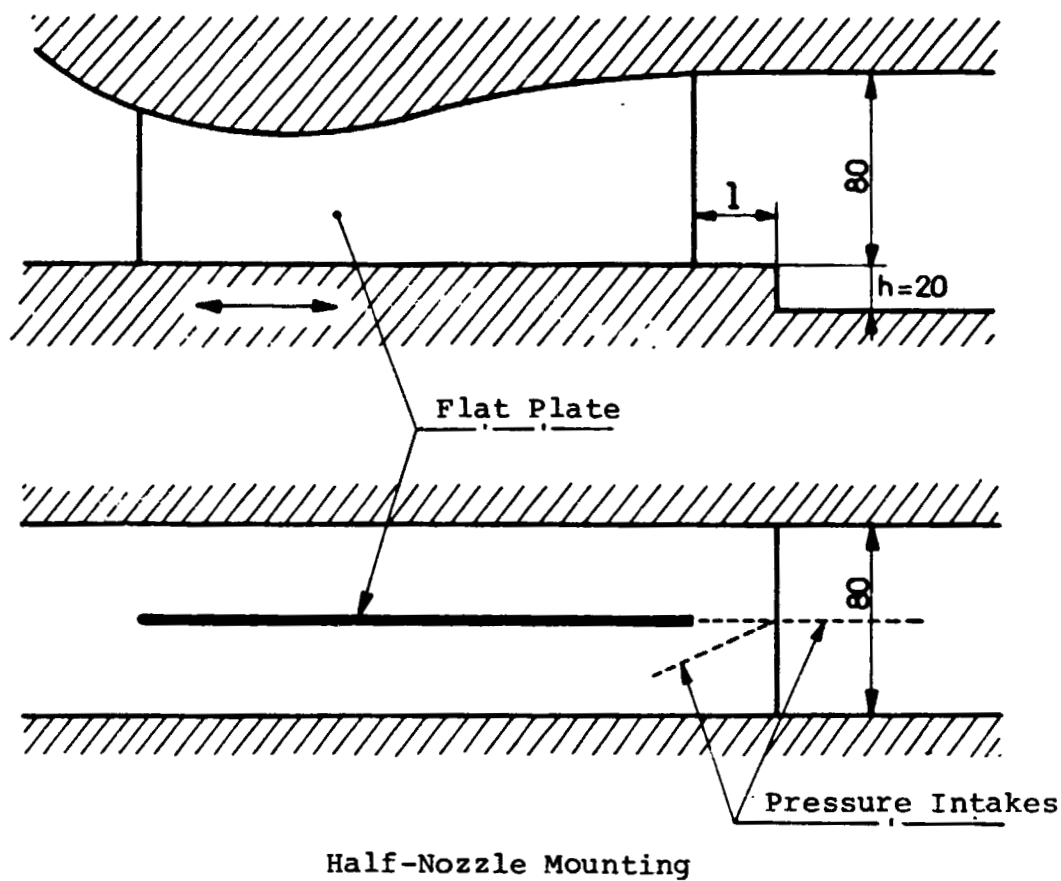
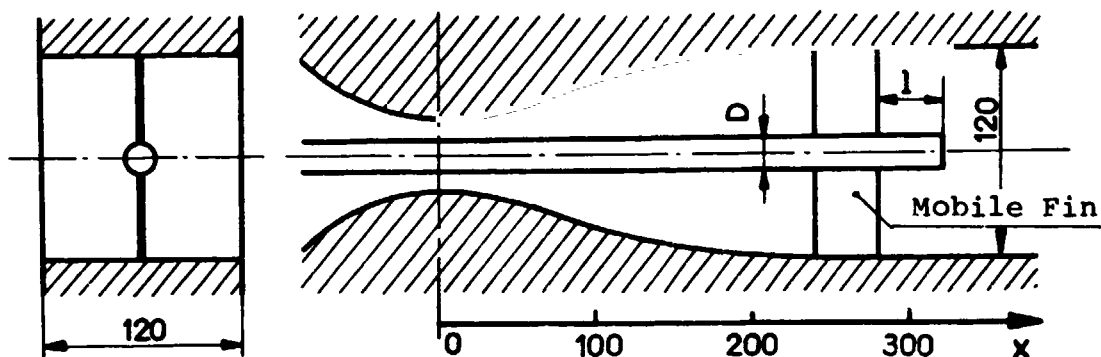
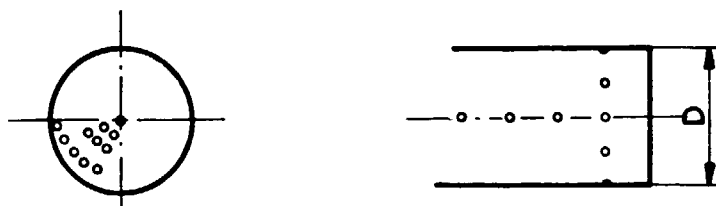


Figure 1 - Interactions On A Base In A Plane
Parallel Flow ($M = 2$).



Mounting Diagram



Pressure Intakes On The Base

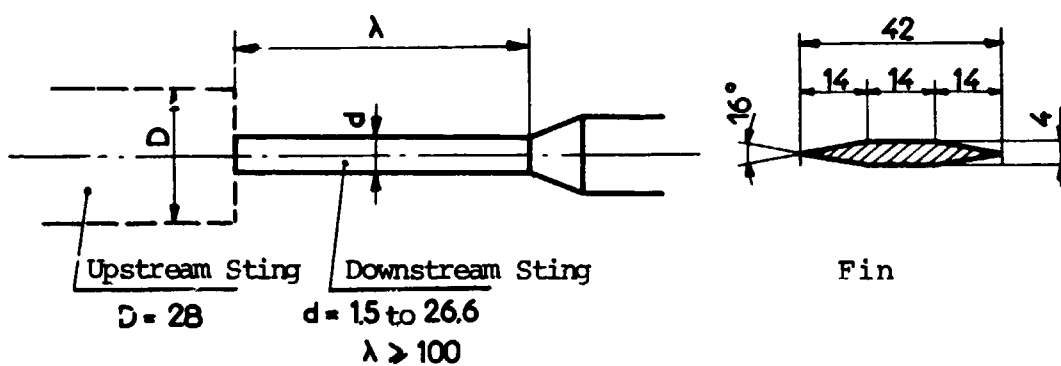


Figure 2 - Interactions Of An Obstacle On The
Base Of A Body Of Revolution.

ORIGINAL PAGE IS
OF POOR QUALITY

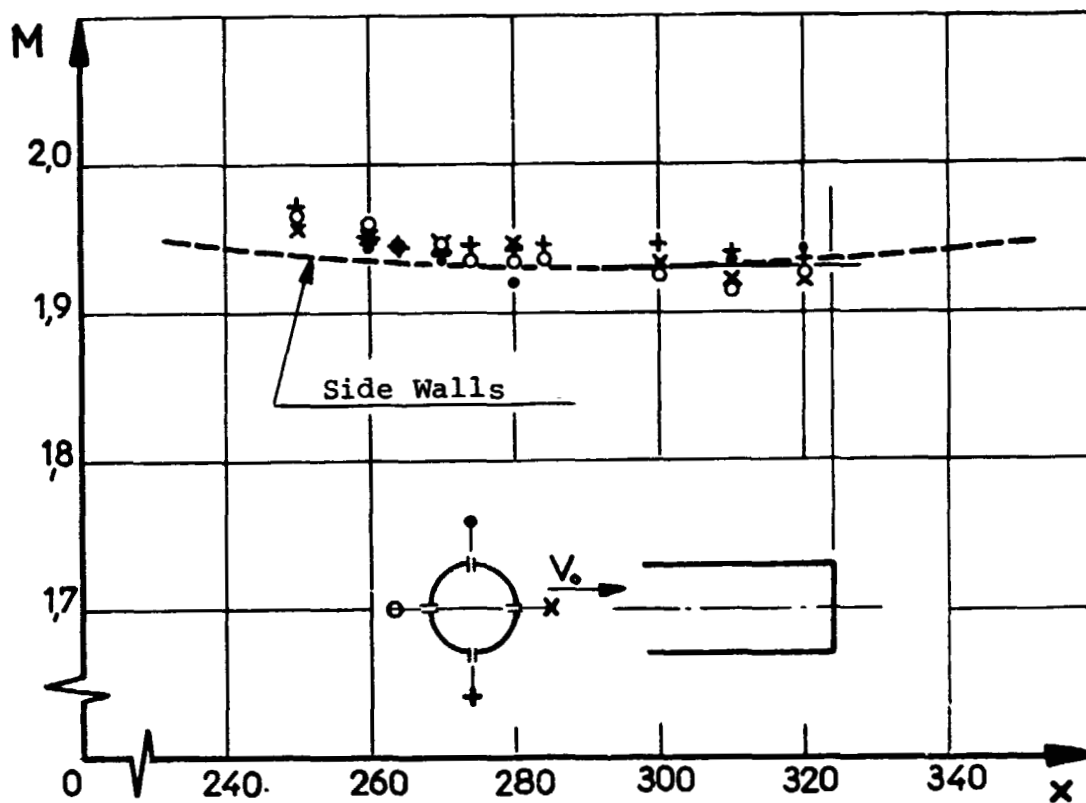


Figure 3 - Local Mach Numbers On The Generatrices Of
A Body Of Revolution.

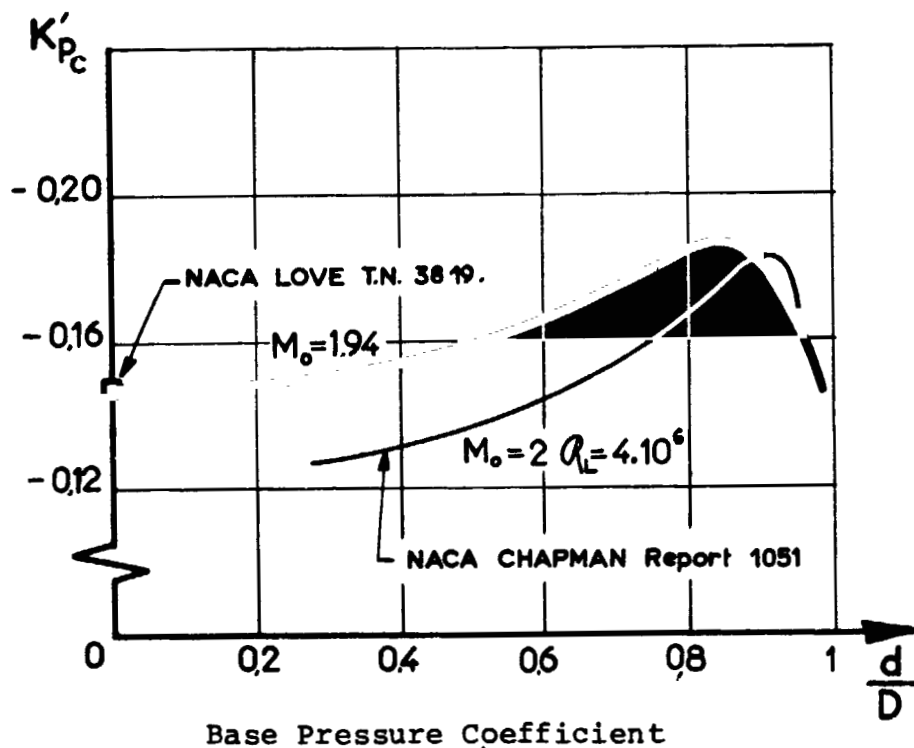
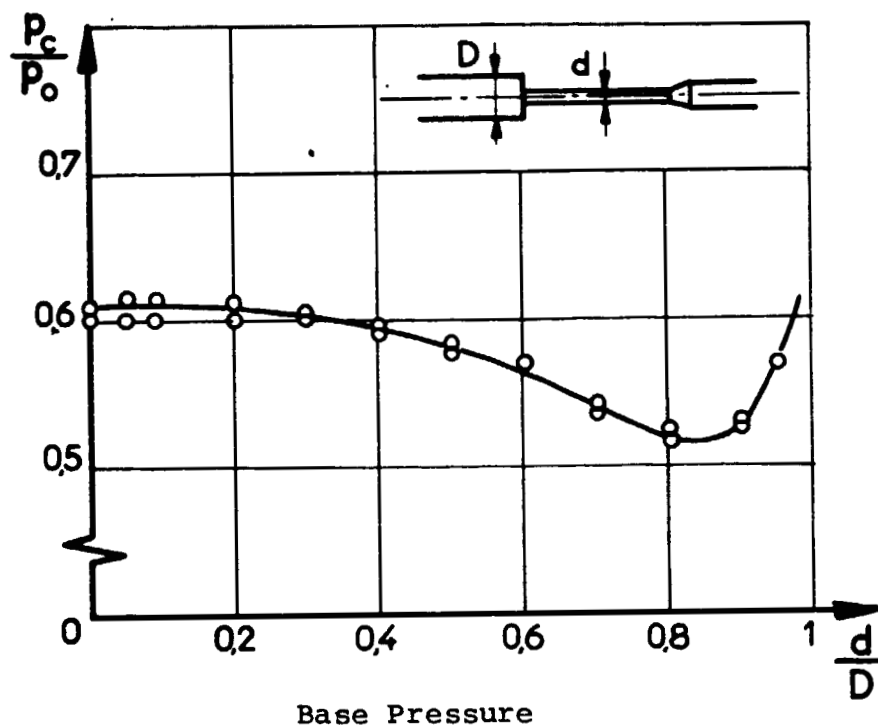


Figure 4 - Interferences Of A Sting On The Base
Of A body Of Revolution With A Turbulent
Boundary Layer (Equivalent $R_x = 3.5 \times 10^6$)

ORIGINAL PAGE IS
OF POOR QUALITY

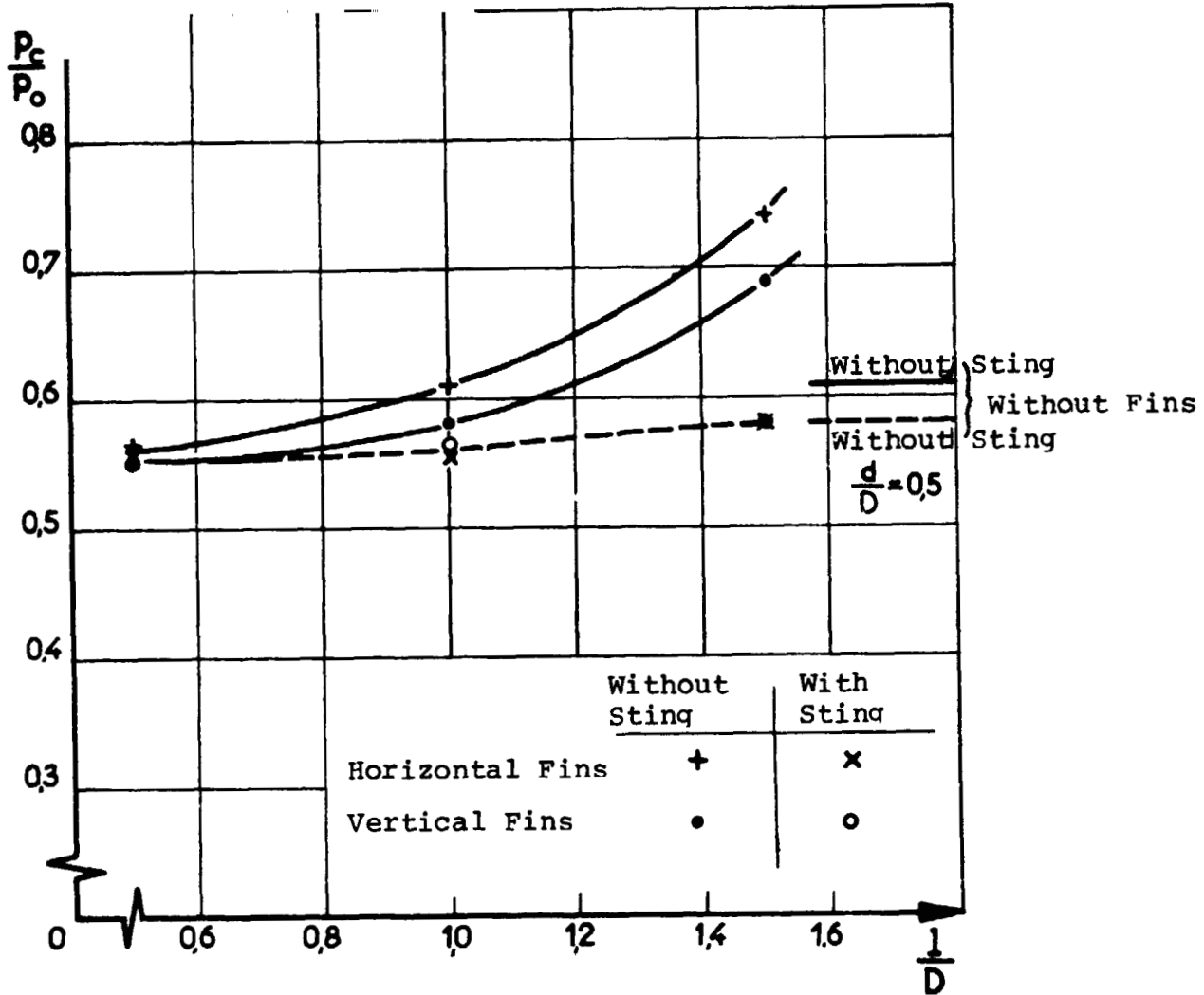
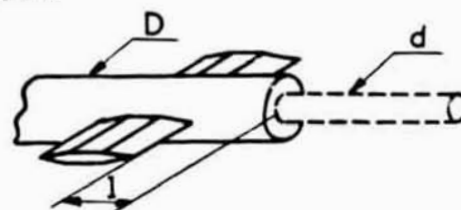


Figure 5 - Interference of A Finned Support On A Body Of Revolution.

$$M_o = 1.94$$

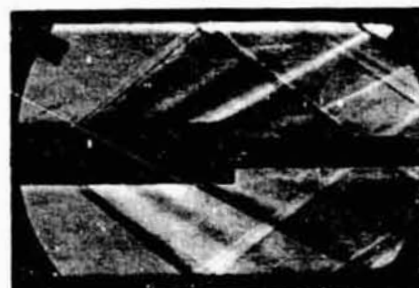
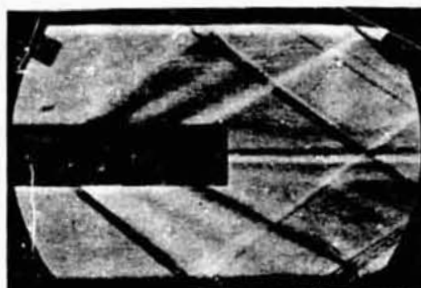
Turbulent Boundary
Layer



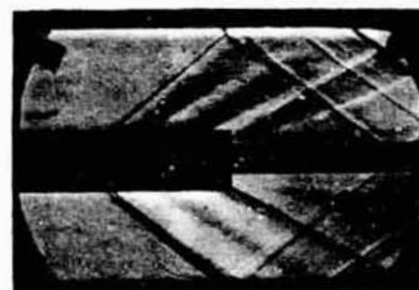
Without Sting

With Sting ($\frac{d}{D} = 0.5$)

$$\frac{l}{D} = 1.5$$



$$\frac{l}{D} = 1$$



$$\frac{l}{D} = 0.5$$

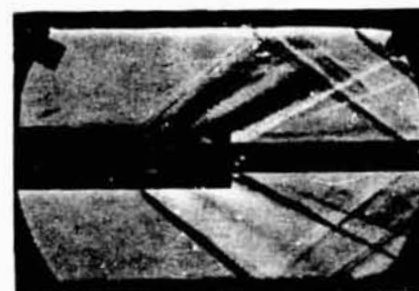


Figure 6 - Strioscopies Of The Flow For Different
Fin Positions.

ORIGINAL PAGE IS
OF POOR QUALITY

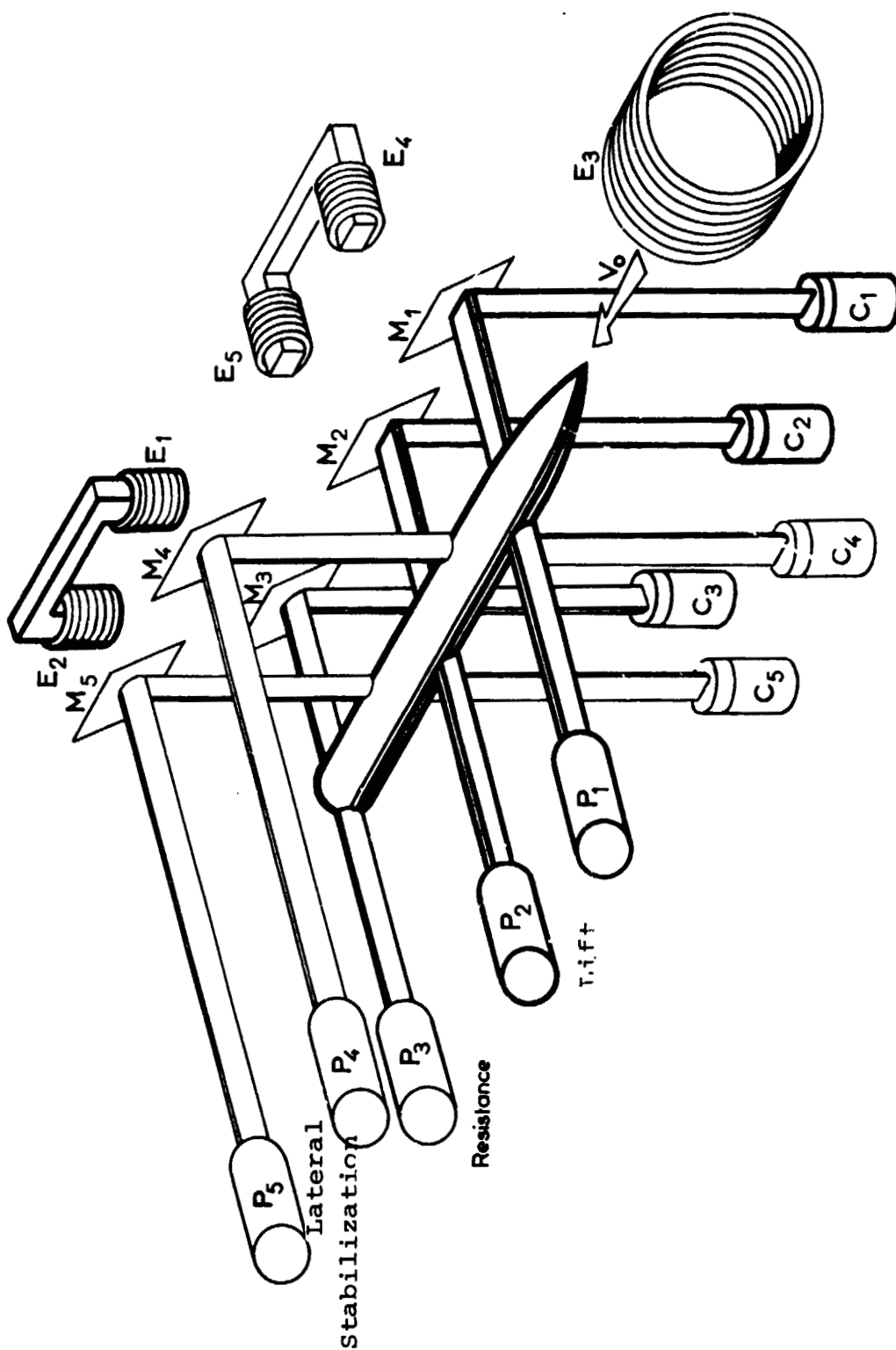


Figure 7 - Diagram Of the ONERA Magnetic Suspension

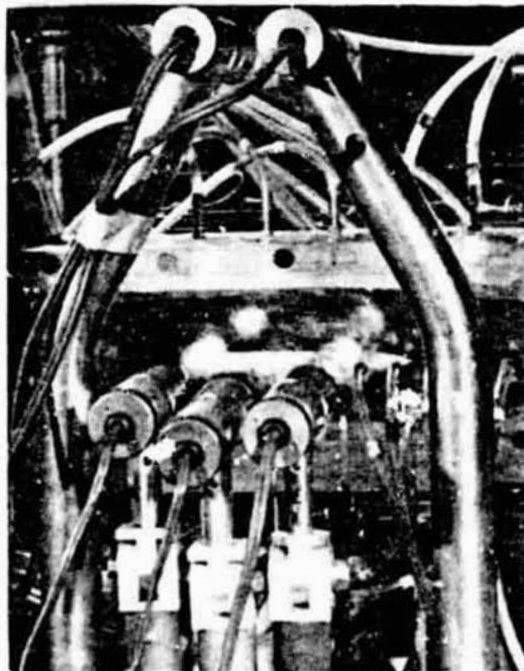
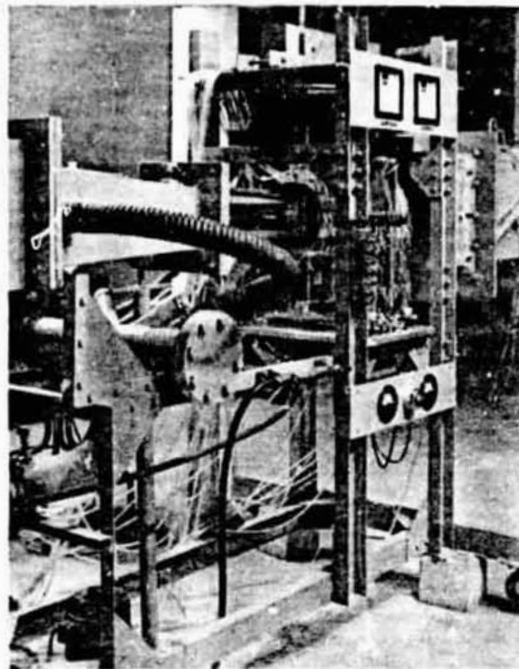


Figure 8 - Supersonic Test Section
With Magnetic Suspension.

ORIGINAL PAGE IS
OF POOR QUALITY

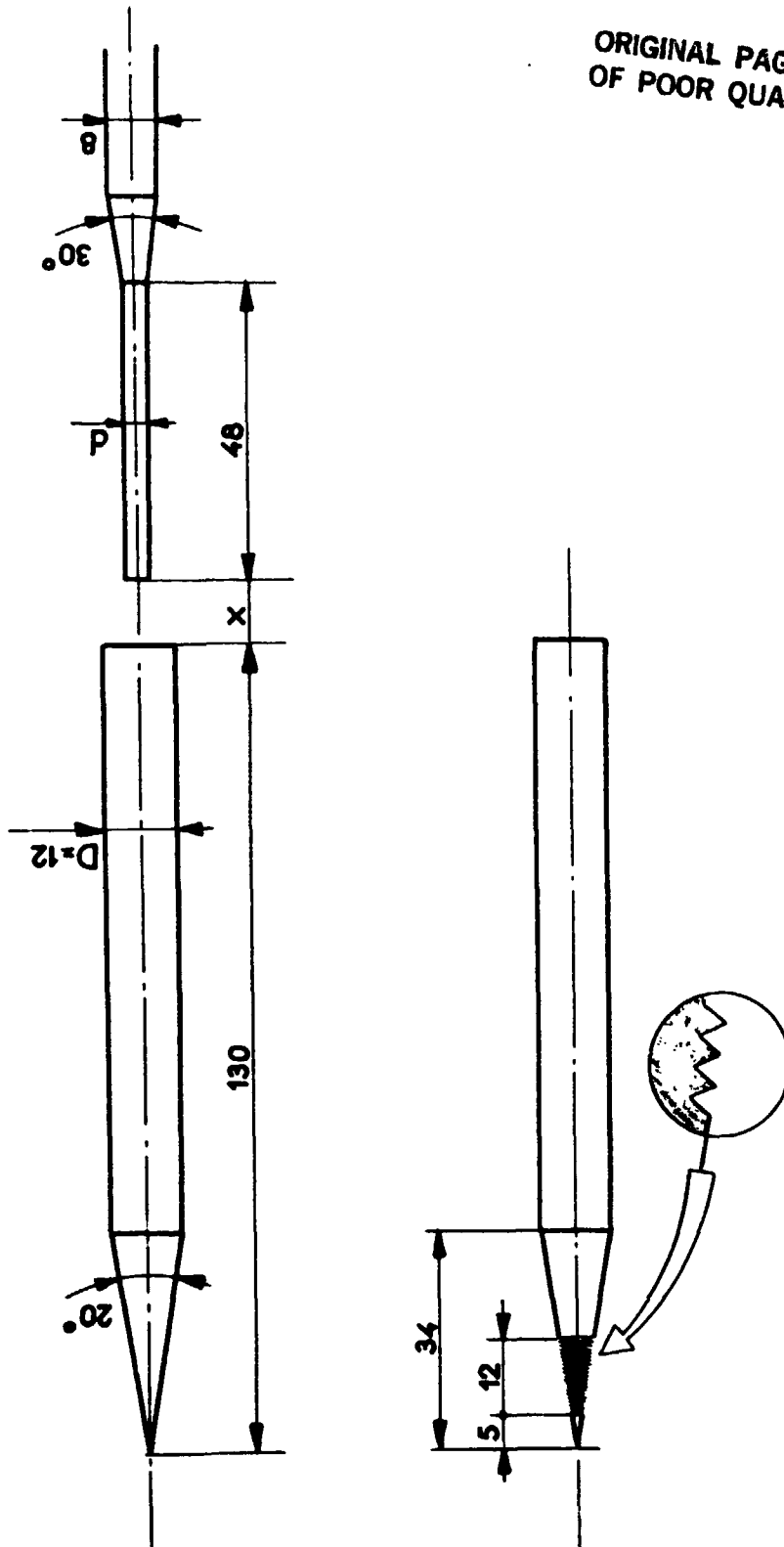


Figure 9 - Transition Initiator (40 Throats, Pitch 0.2)
Test Mock-Up And Sting.

$$M_0 = 2.42 \quad \alpha_L = 1.4 \cdot 10^\circ$$

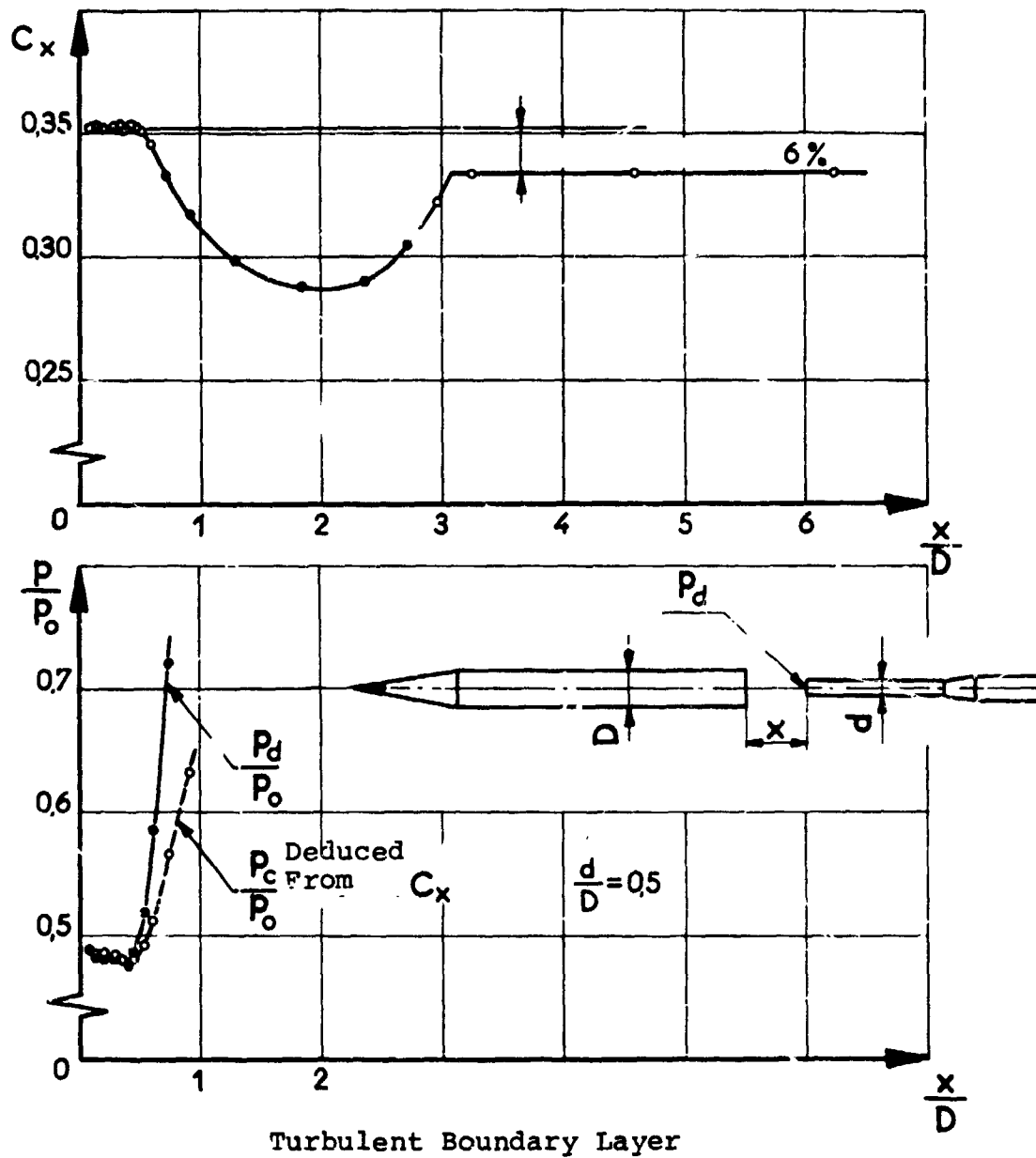
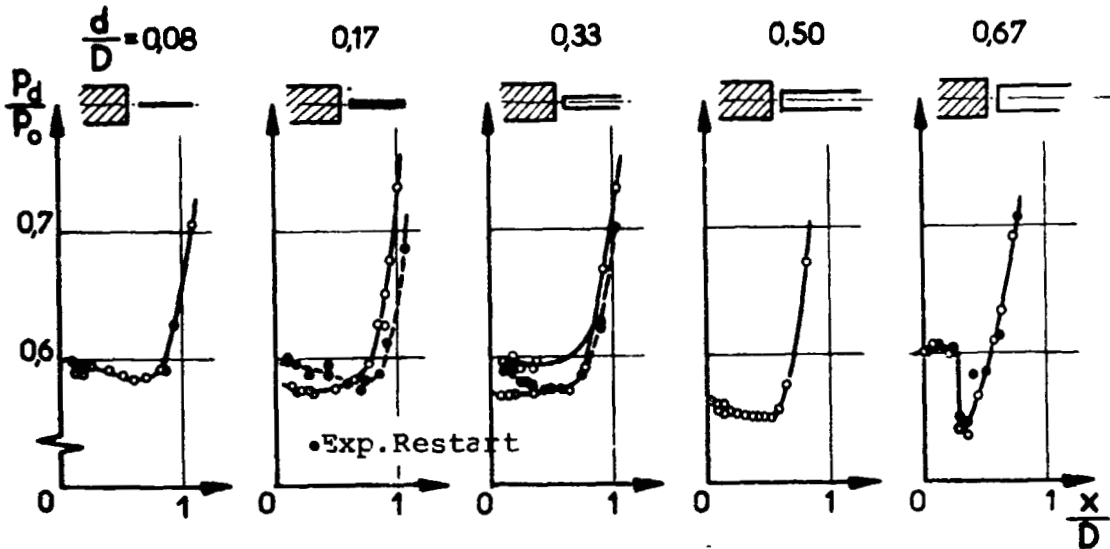
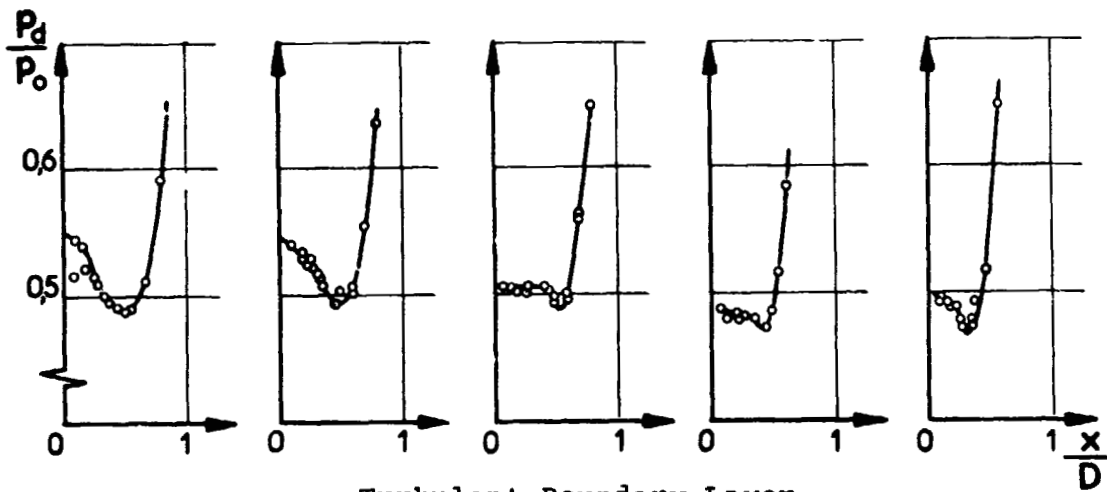
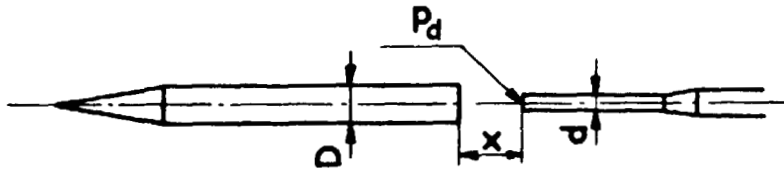


Figure 10 - Interference Of A Sting

$$M_o = 2,42 \quad R_L = 1,4 \cdot 10^6$$

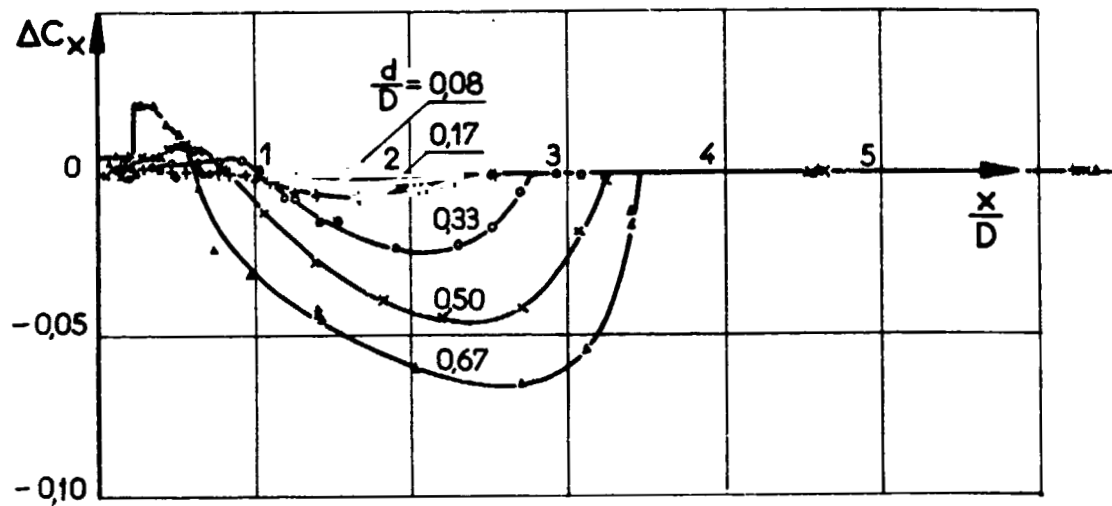


Laminar Boundary Layer

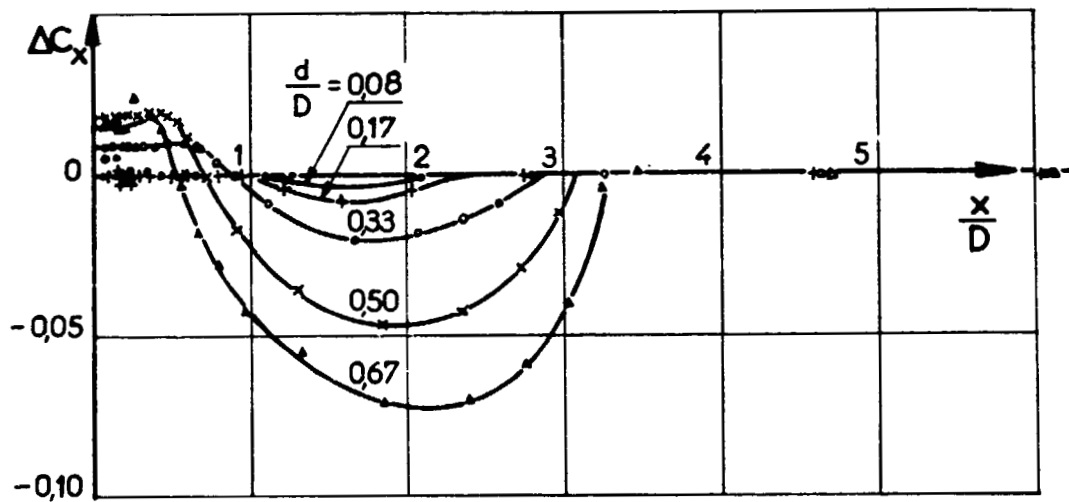


Turbulent Boundary Layer

Figure 11 - Pressure Variations At The Tip Of
A Sting.



Laminar Boundary Layer



Turbulent Boundary Layer

Figure 12 - Variation Of A Sting On The
Resistance Coefficient C_x .

OR. VAL PAGE IS
OF POOR QUALITY

$$M_0 = 2.42 \quad R_L = 1.4 \cdot 10^6$$

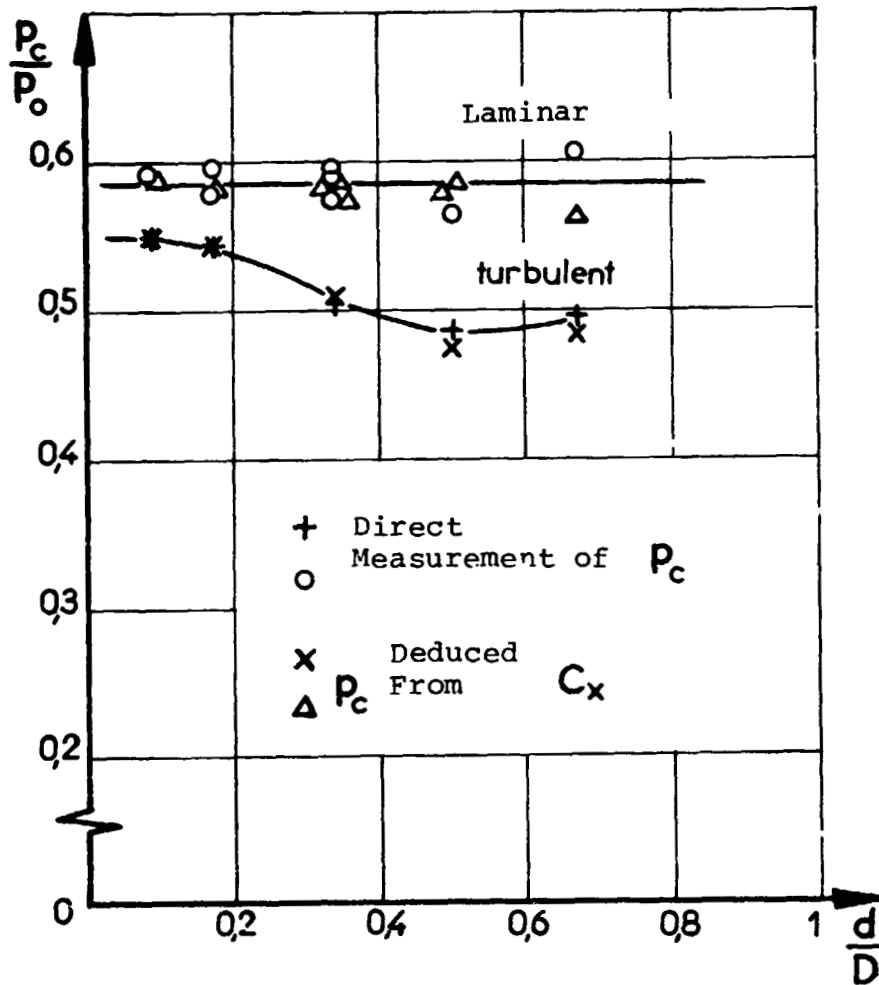


Figure 13 - Interference Of A Sting
On The Base Pressure

$$M_0 = 2.42 \quad R_L = 1.4 \cdot 10^6$$

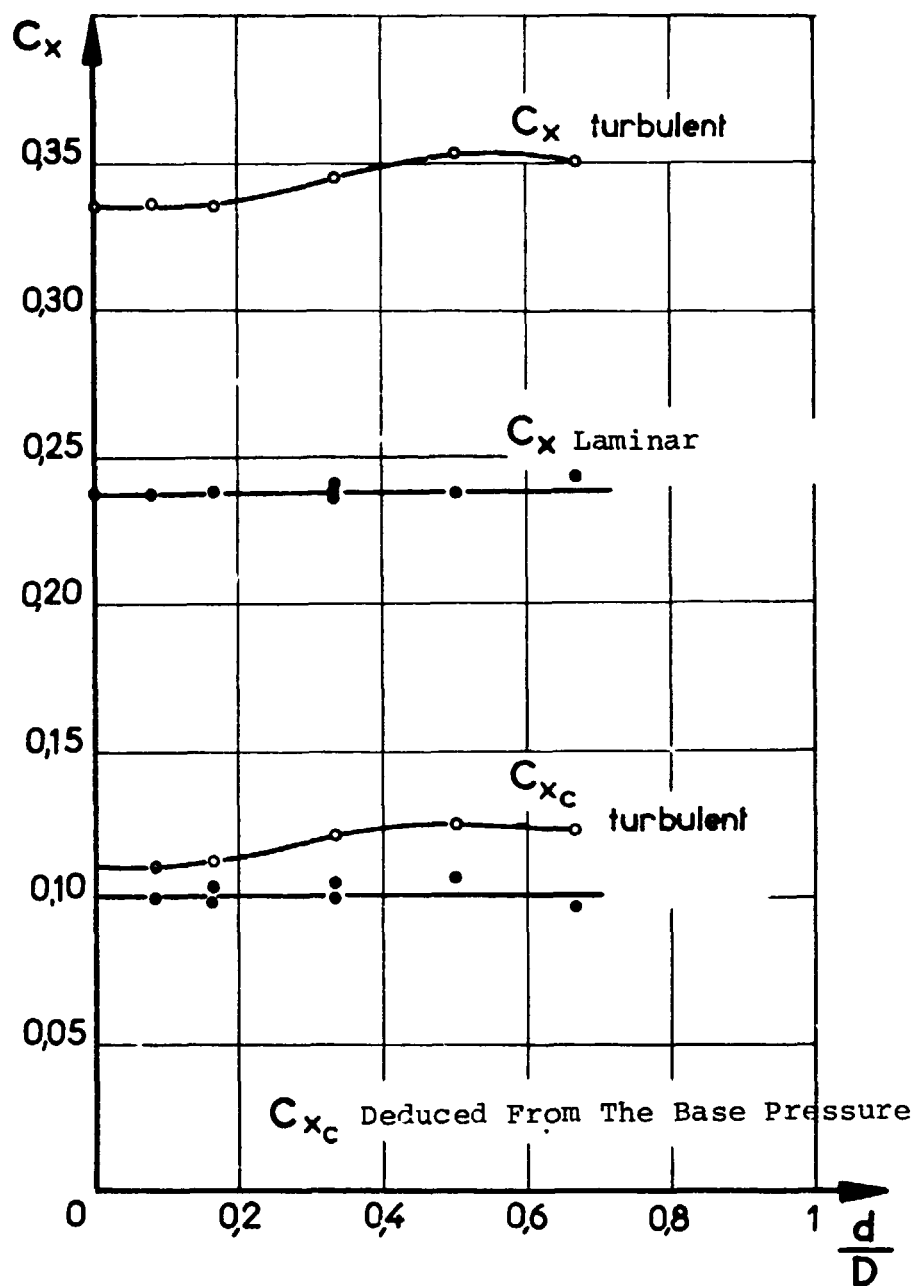


Figure 14 - Results With The Conical-Cylindrical Model

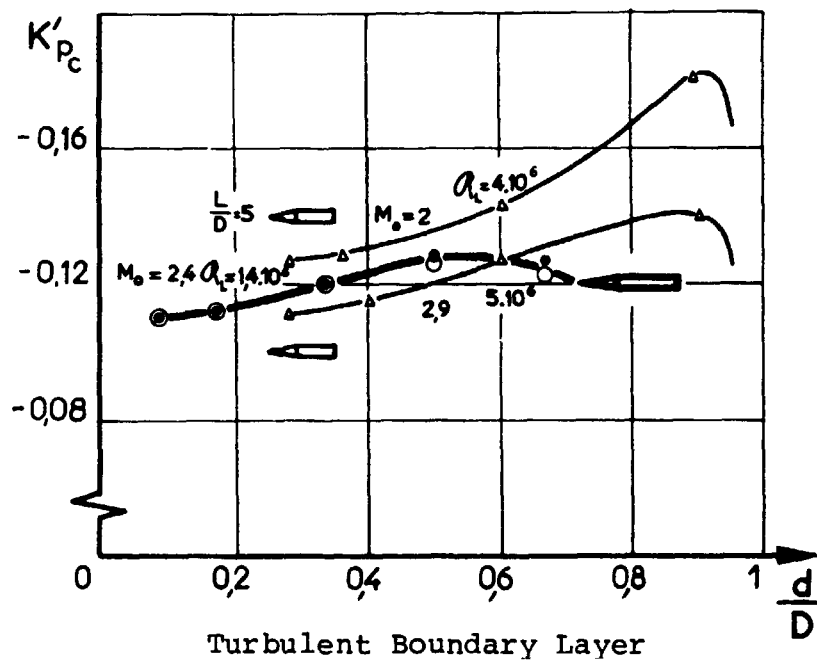
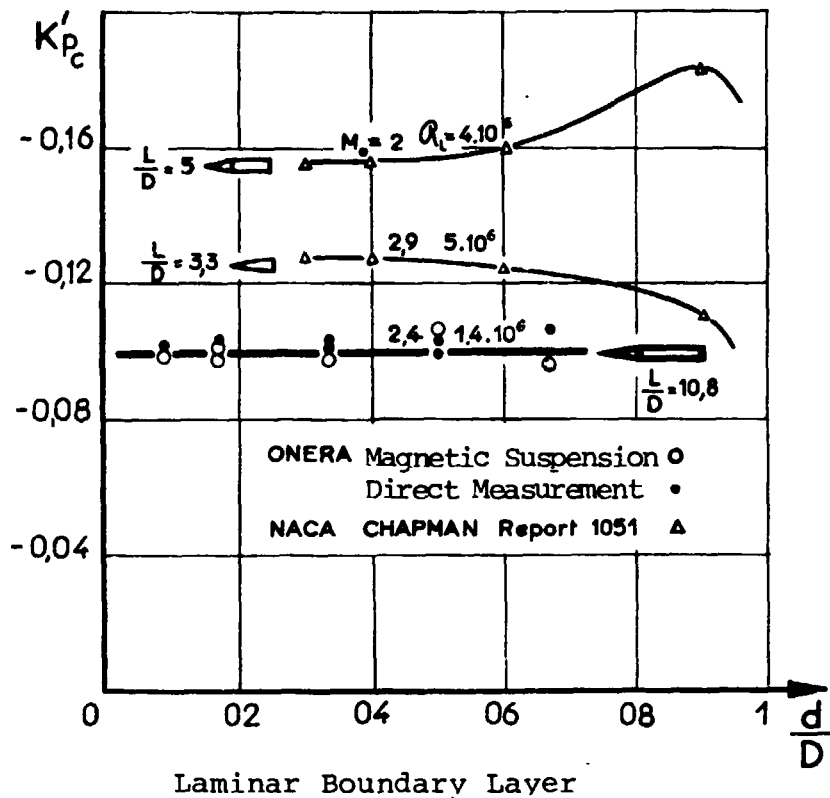
ORIGINAL PAGE IS
OF POOR QUALITY

Figure 15 - Base Pressure Coefficient With
Respect To The Relative Sting Diameter.

ORIGINAL PAGE IN
OF POOR QUALITY

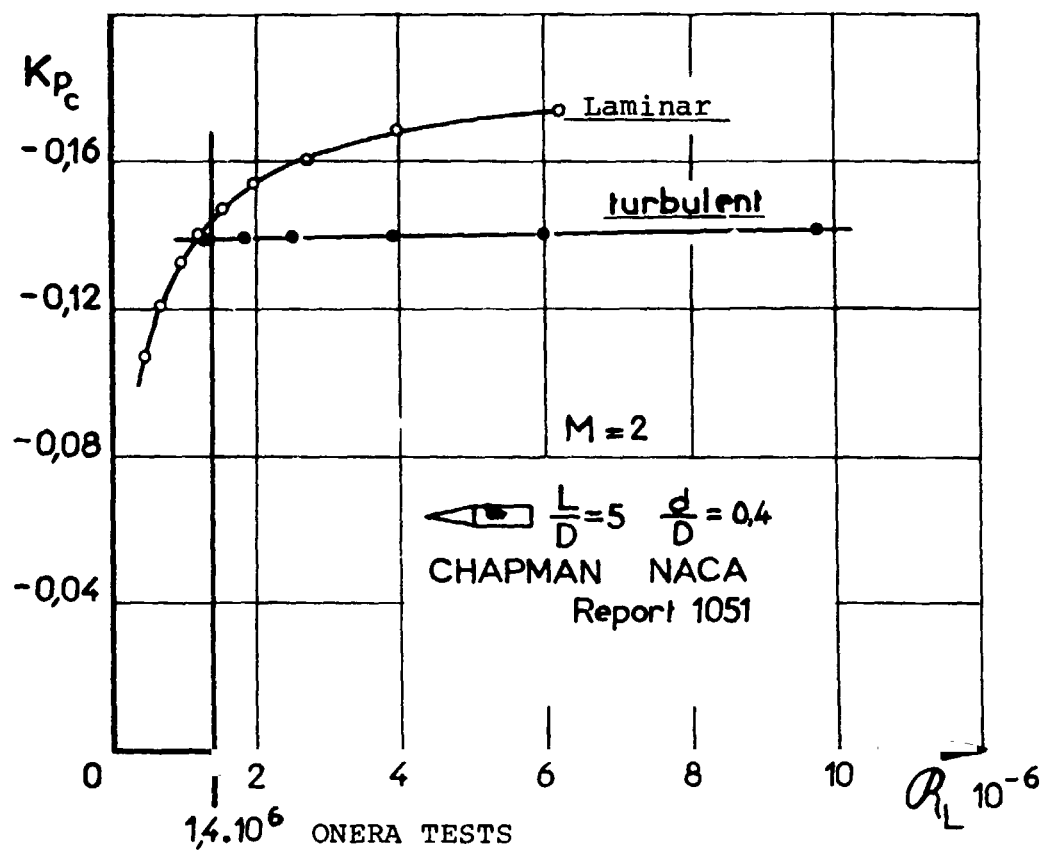


Figure 16 - Effect Of The
Reynolds Number